Supplementary Material for **Genomic traits and social determinants of health drive bacterial antimicrobial resistance: current trends and projections to 2050**

Alexandre Maciel-Guerra[1‡], Michelle Baker[1‡], Ruoqi Wang[2‡], Luo Chengchang[2], Yan Xu[2], Enzo Guerrero-Araya[2], Weihua Meng[2], Ge Wu[2], Komkiew Pinpimai[1], Nicola Senin[3], Tania Dottorini[1,2]*

*Corresponding author (tania.dottorini@nottingham.ac.uk)

‡ These authors contributed equally

Contents:

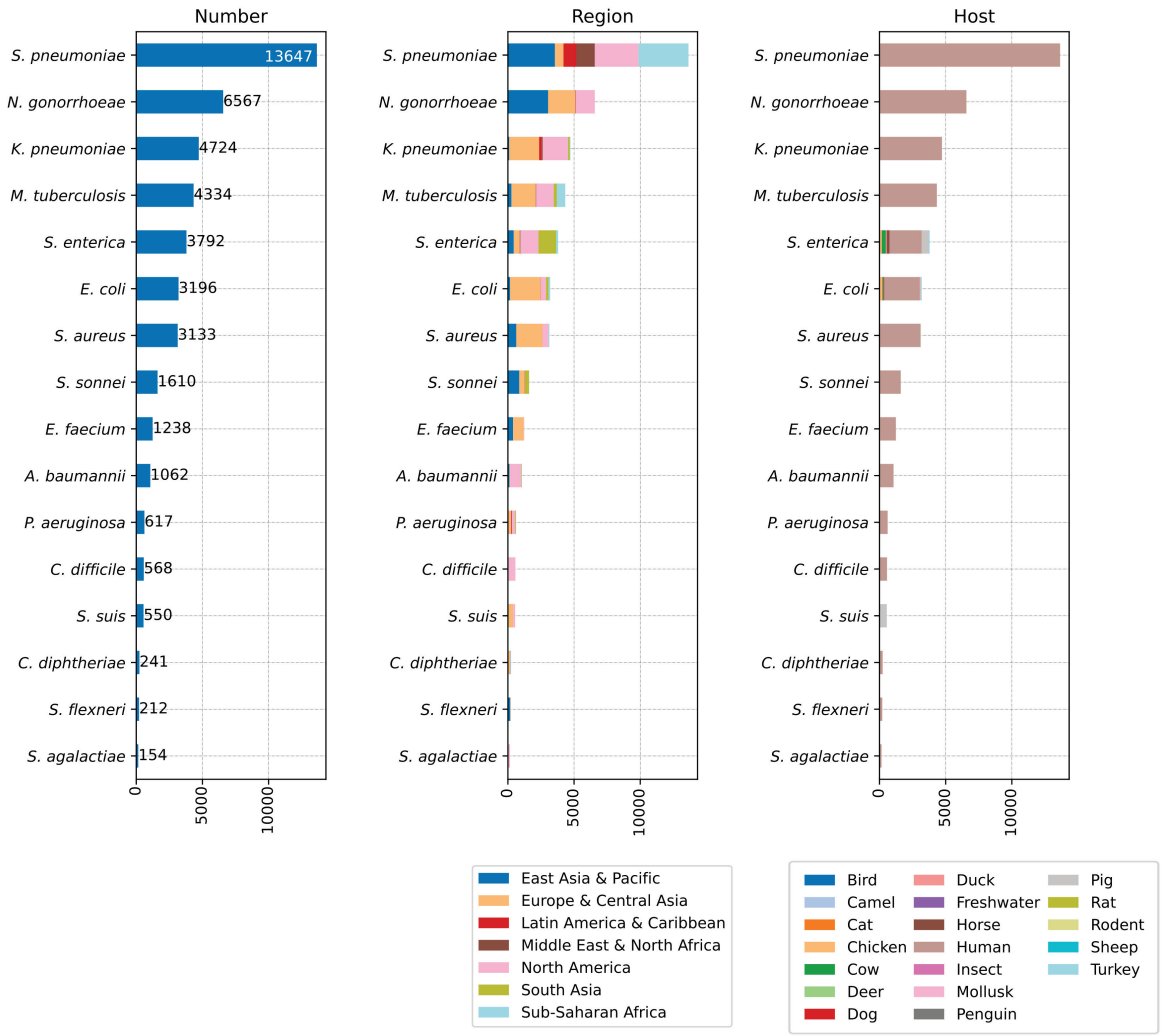

Figure S1. Bar plots showing distribution of isolates selected for analysis from BV-BRC database. Bacterial species were included if there were more than 100 high quality DNA sequences with accompanying resistance/susceptibility profiles in the database (see Methods). (a) Number of isolates per bacterial species. (b) Region of origin for included isolates, bars coloured by World Bank regions. (c) Host of isolates, bars colours by host.

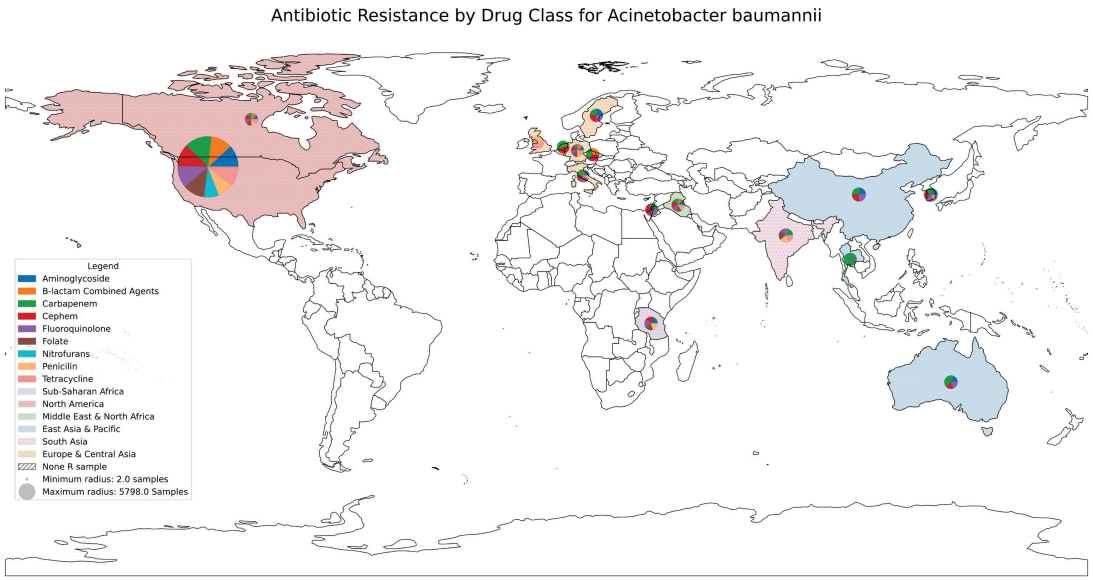

Figure S2. Geographic distributions of 1063 *A. baumannii* isolates with 12,074 associated resistance susceptibility phenotypic profiles obtained from the BV-BRC database[1].The pie chart on each country shows the proportion of resistance profiles for by class for each country, with the size of the chart indicating the overall number of genomes. The world map[2] has been divided according to the seven World Bank regions (East Asia and Pacific; Europe and Central Asia; Latin America and Caribbean; Middle East and North Africa; North America; South Asia; Sub-Saharan Africa).

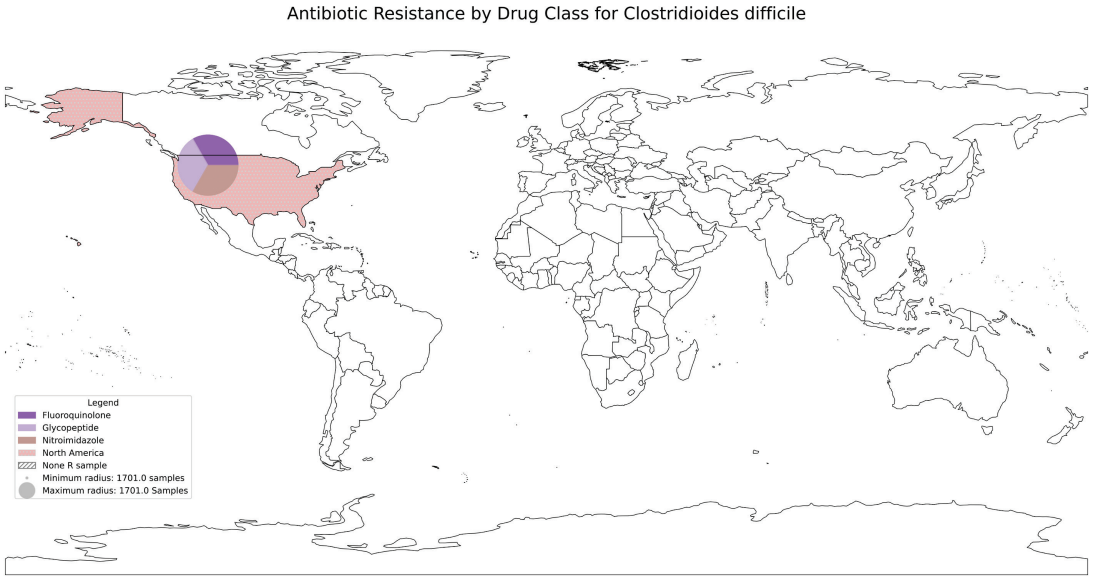

Figure S3. Geographic distributions of 568 *C. difficile* isolates with 1,701 associated resistance susceptibility phenotypic profiles obtained from the BV-BRC database[1].The pie chart on each country shows the proportion of resistance profiles for by class for each country, with the size of the chart indicating the overall number of genomes. The world map[2] has been divided according to the seven World Bank regions (East Asia and Pacific; Europe and Central Asia; Latin America and Caribbean; Middle East and North Africa; North America; South Asia; Sub-Saharan Africa).

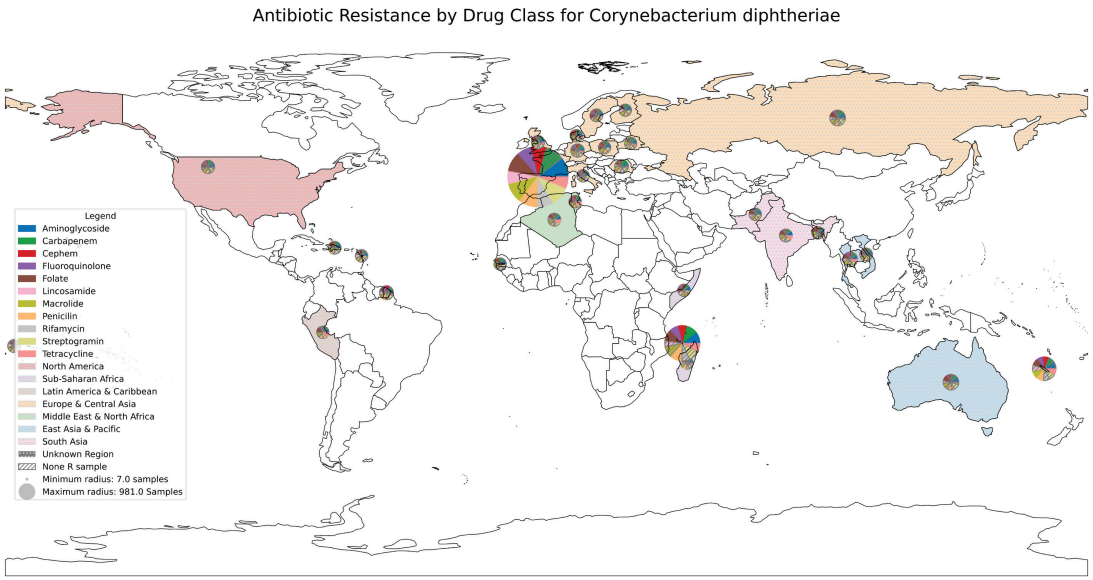

Figure S4. Geographic distributions of 214 *C. diphtheriae* isolates with 3,899 associated resistance susceptibility phenotypic profiles obtained from the BV-BRC database[1].The pie chart on each country shows the proportion of resistance profiles for by class for each country, with the size of the chart indicating the overall number of genomes. The world map[2] has been divided according to the seven World Bank regions (East Asia and Pacific; Europe and Central Asia; Latin America and Caribbean; Middle East and North Africa; North America; South Asia; Sub-Saharan Africa).

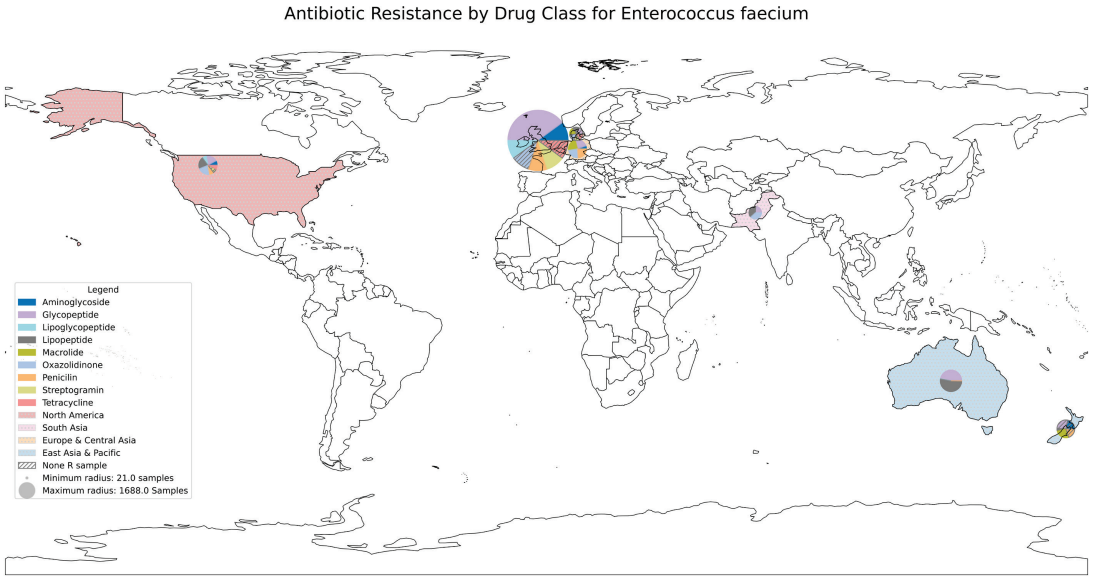

Figure S5. Geographic distributions of 1238 *E. faecium* isolates with 2,960 associated resistance susceptibility phenotypic profiles obtained from the BV-BRC database[1].The pie chart on each country shows the proportion of resistance profiles for by class for each country, with the size of the chart indicating the overall number of genomes. The world map[2] has been divided according to the seven World Bank regions (East Asia and Pacific; Europe and Central Asia; Latin America and Caribbean; Middle East and North Africa; North America; South Asia; Sub-Saharan Africa).

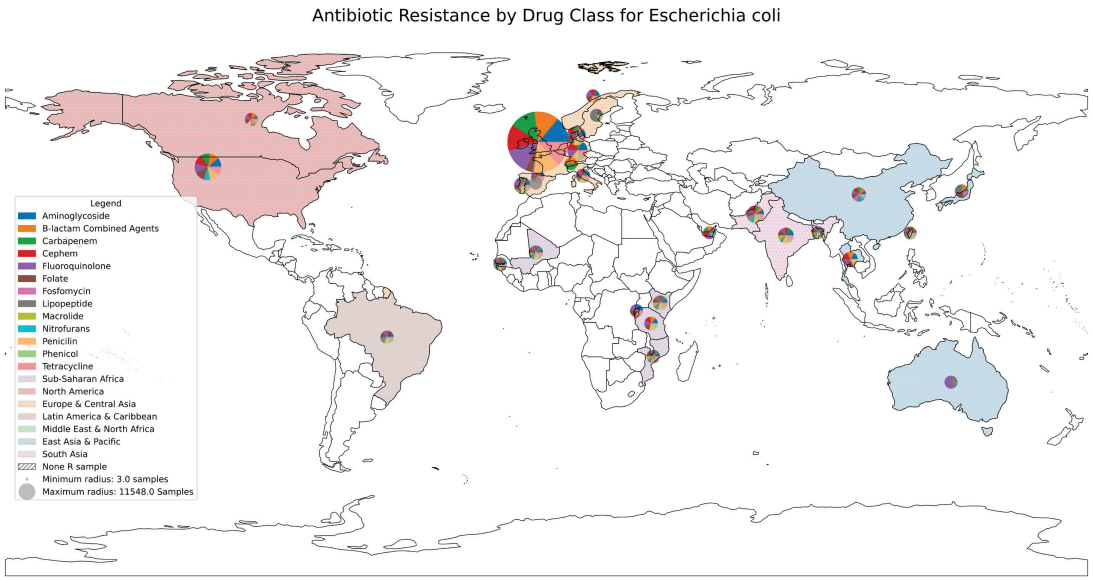

Figure S6. Geographic distributions of 3196 *E. coli* isolates with 39,855 associated resistance susceptibility phenotypic profiles obtained from the BV-BRC database[1].The pie chart on each country shows the proportion of resistance profiles for by class for each country, with the size of the chart indicating the overall number of genomes. The world map[2] has been divided according to the seven World Bank regions (East Asia and Pacific; Europe and Central Asia; Latin America and Caribbean; Middle East and North Africa; North America; South Asia; Sub-Saharan Africa).

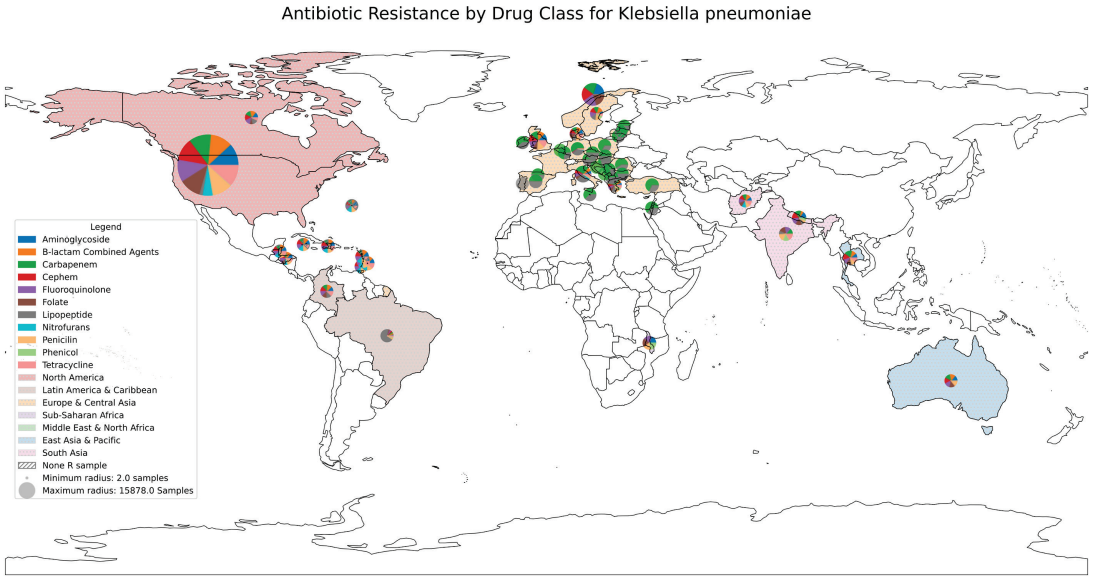

Figure S7. Geographic distributions of 4724 *K. pneumoniae* isolates with 51,896 associated resistance susceptibility phenotypic profiles obtained from the BV-BRC database[1].The pie chart on each country shows the proportion of resistance profiles for by class for each country, with the size of the chart indicating the overall number of genomes. The world map[2] has been divided according to the seven World Bank regions (East Asia and Pacific; Europe and Central Asia; Latin America and Caribbean; Middle East and North Africa; North America; South Asia; Sub-Saharan Africa).

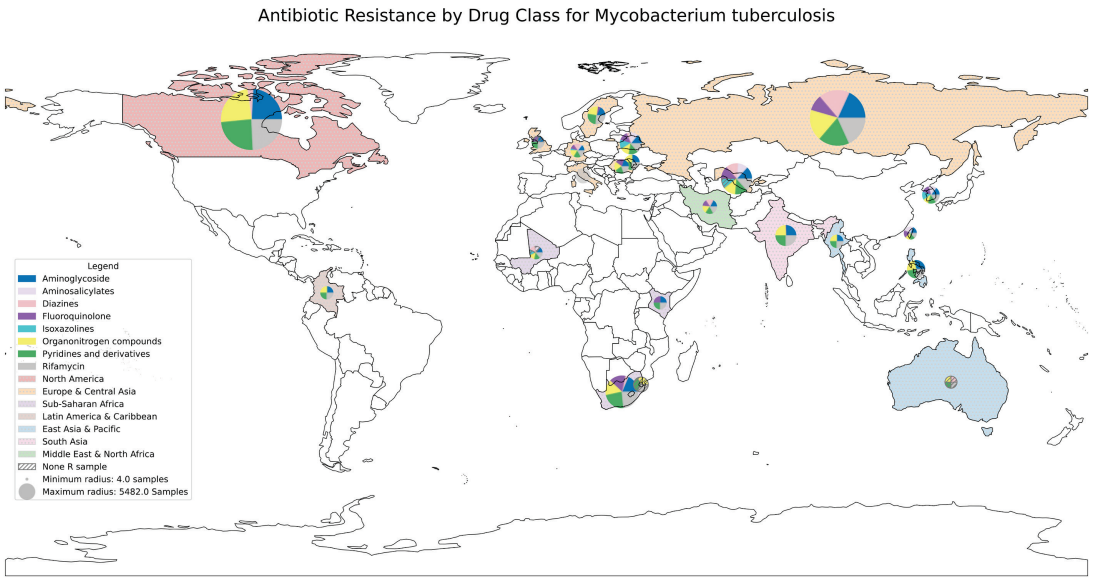

Figure S8. Geographic distributions of 4334 *M. tuberculosis* isolates with 24,710 associated resistance susceptibility phenotypic profiles obtained from the BV-BRC database[1].The pie chart on each country shows the proportion of resistance profiles for by class for each country, with the size of the chart indicating the overall number of genomes. The world map[2] has been divided according to the seven World Bank regions (East Asia and Pacific; Europe and Central Asia; Latin America and Caribbean; Middle East and North Africa; North America; South Asia; Sub-Saharan Africa).

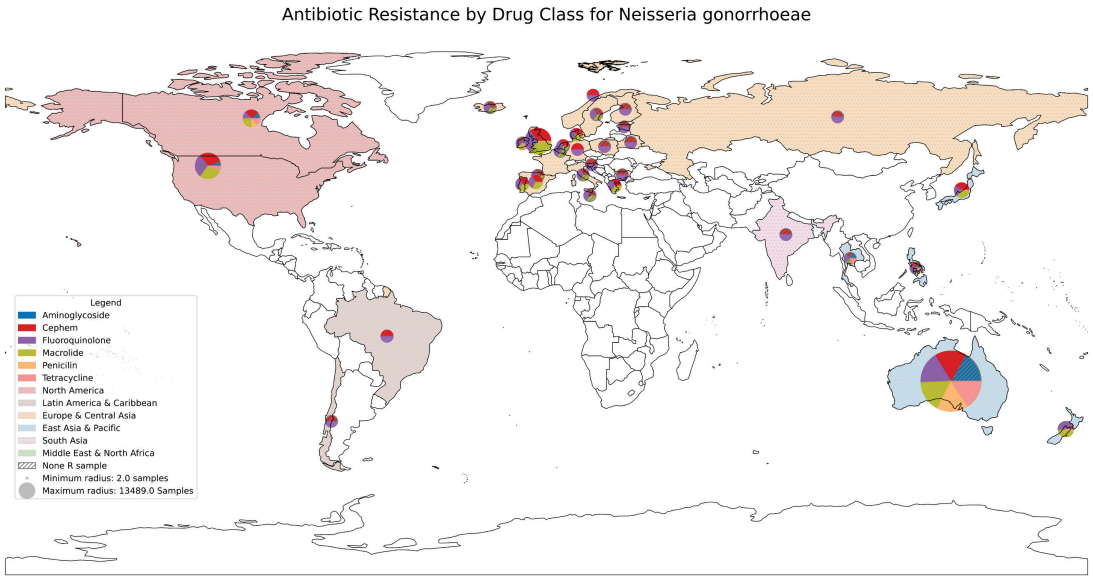

Figure S9. Geographic distributions of 6567 *N. gonorrhoeae* isolates with 30,741 associated resistance susceptibility phenotypic profiles obtained from the BV-BRC database[1].The pie chart on each country shows the proportion of resistance profiles for by class for each country, with the size of the chart indicating the overall number of genomes. The world map[2] has been divided according to the seven World Bank regions (East Asia and Pacific; Europe and Central Asia; Latin America and Caribbean; Middle East and North Africa; North America; South Asia; Sub-Saharan Africa).

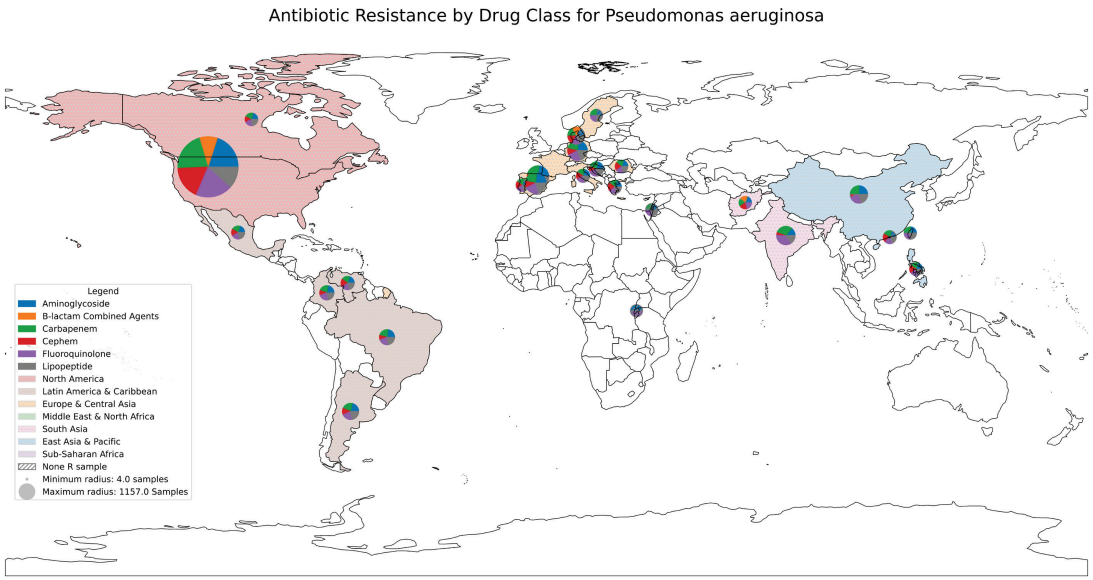

Figure S10. Geographic distributions of 617 *P. aeruginosa* isolates with 3,531 associated resistance susceptibility phenotypic profiles obtained from the BV-BRC database[1].The pie chart on each country shows the proportion of resistance profiles for by class for each country, with the size of the chart indicating the overall number of genomes. The world map[2] has been divided according to the seven World Bank regions (East Asia and Pacific; Europe and Central Asia; Latin America and Caribbean; Middle East and North Africa; North America; South Asia; Sub-Saharan Africa).

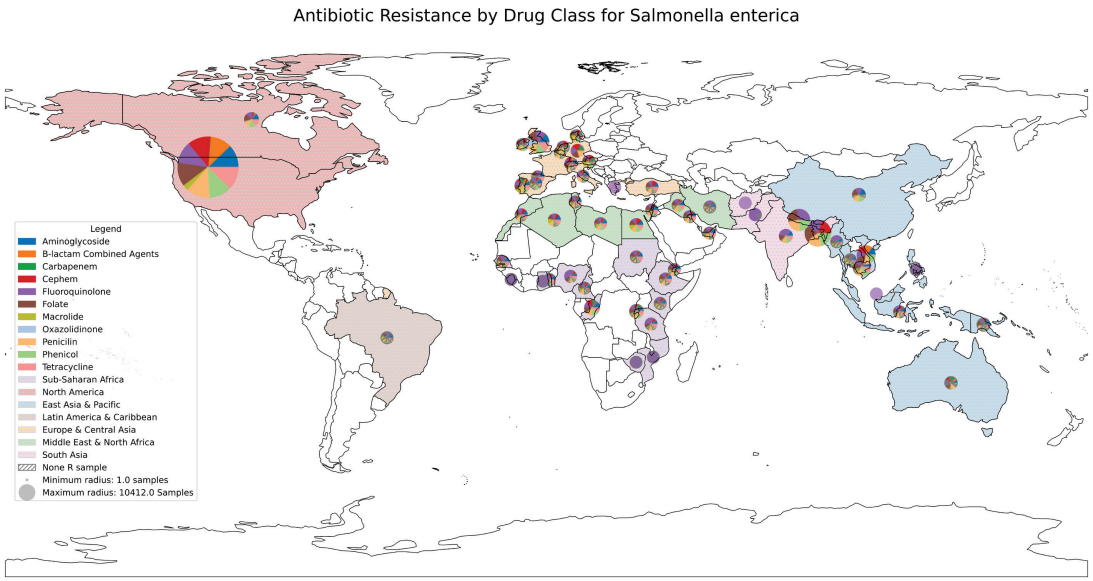

Figure S11. Geographic distributions of 3792 *S. enterica* isolates with 33,562 associated resistance susceptibility phenotypic profiles obtained from the BV-BRC database[1].The pie chart on each country shows the proportion of resistance profiles for by class for each country, with the size of the chart indicating the overall number of genomes. The world map[2] has been divided according to the seven World Bank regions (East Asia and Pacific; Europe and Central Asia; Latin America and Caribbean; Middle East and North Africa; North America; South Asia; Sub-Saharan Africa).

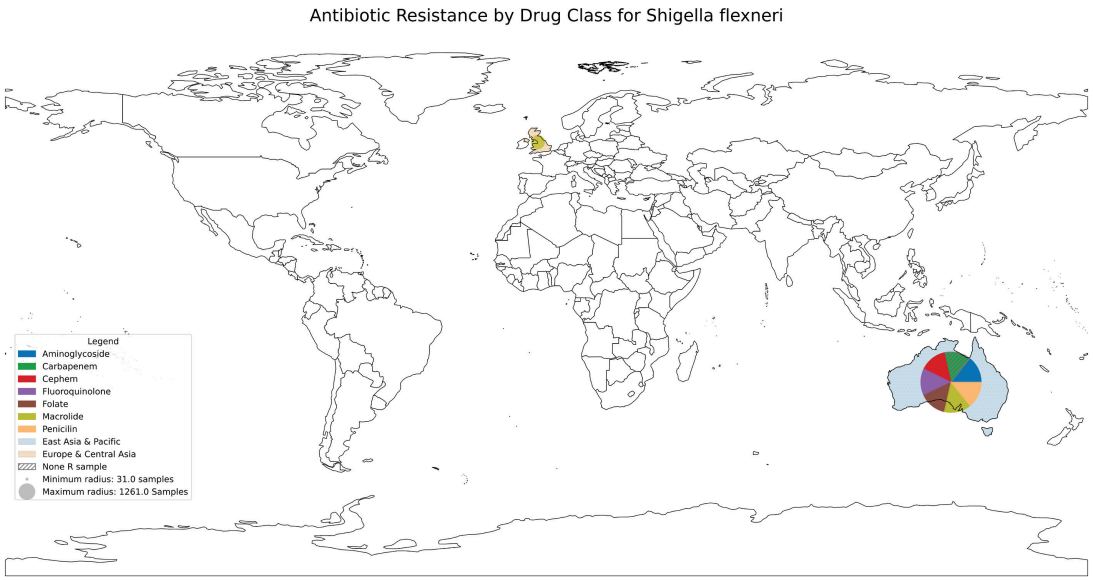

Figure S12. Geographic distributions of 212 *S. flexneri* isolates with 1,473 associated resistance susceptibility phenotypic profiles obtained from the BV-BRC database[1].The pie chart on each country shows the proportion of resistance profiles for by class for each country, with the size of the chart indicating the overall number of genomes. The world map[2] has been divided according to the seven World Bank regions (East Asia and Pacific; Europe and Central Asia; Latin America and Caribbean; Middle East and North Africa; North America; South Asia; Sub-Saharan Africa).

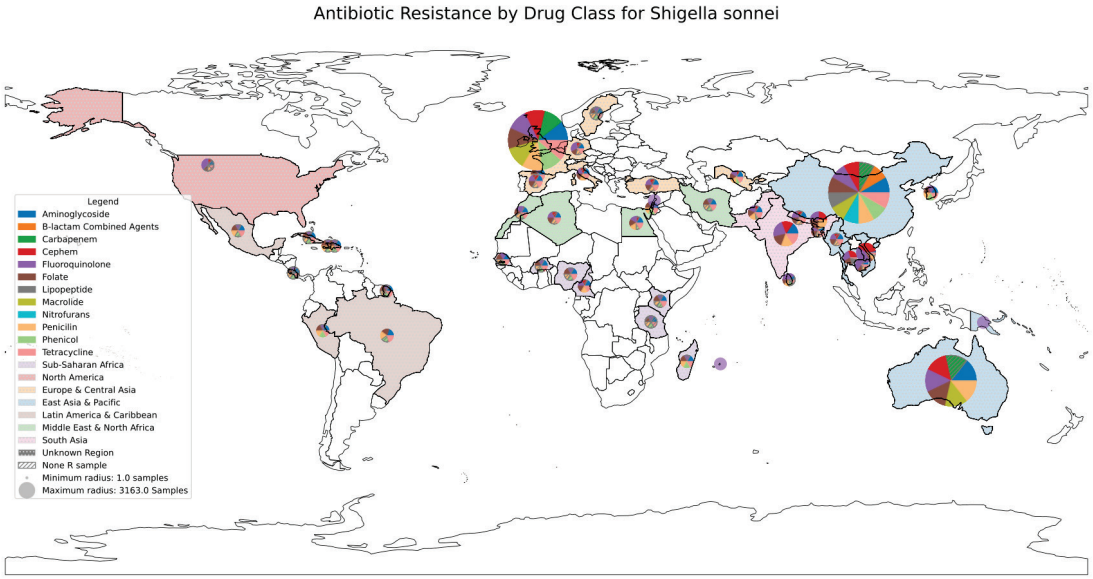

Figure S13. Geographic distributions of 1610 *S. sonnei* isolates with 17,653 associated resistance susceptibility phenotypic profiles obtained from the BV-BRC database[1].The pie chart on each country shows the proportion of resistance profiles for by class for each country, with the size of the chart indicating the overall number of genomes. The world map[2] has been divided according to the seven World Bank regions (East Asia and Pacific; Europe and Central Asia; Latin America and Caribbean; Middle East and North Africa; North America; South Asia; Sub-Saharan Africa).

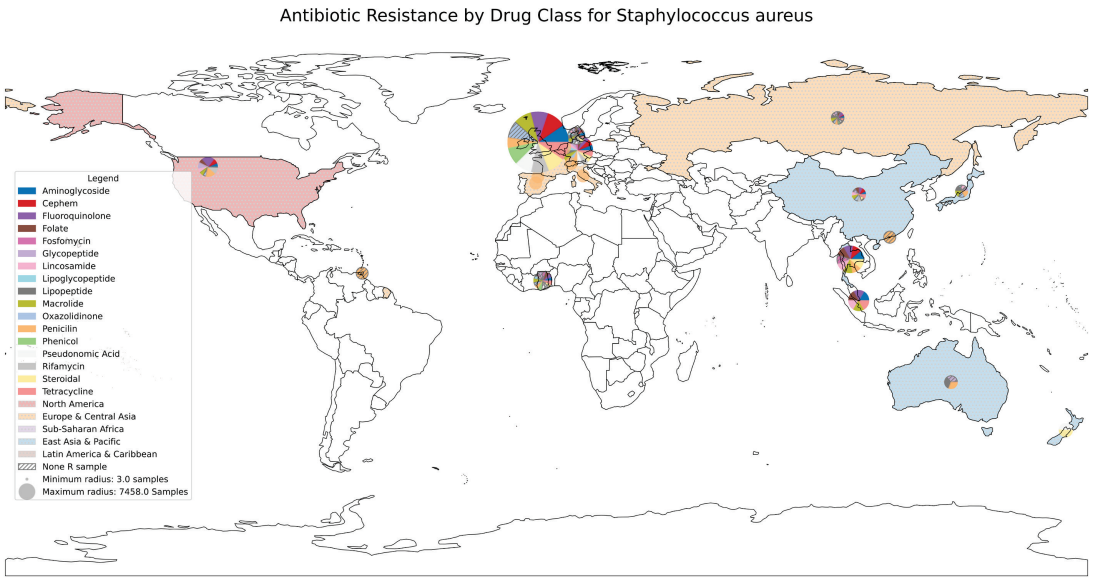

Figure S14. Geographic distributions of 3133 *S. aureus* isolates with 18,839 associated resistance susceptibility phenotypic profiles obtained from the BV-BRC database[1].The pie chart on each country shows the proportion of resistance profiles for by class for each country, with the size of the chart indicating the overall number of genomes. The world map[2] has been divided according to the seven World Bank regions (East Asia and Pacific; Europe and Central Asia; Latin America and Caribbean; Middle East and North Africa; North America; South Asia; Sub-Saharan Africa).

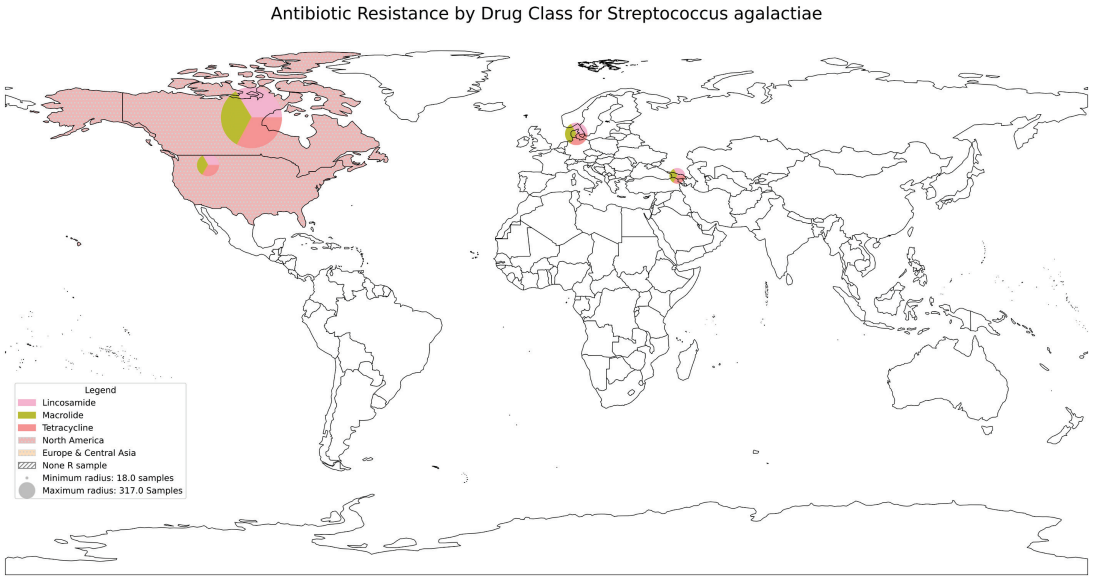

Figure S15. Geographic distributions of 154 *S. agalactiae* isolates with 458 associated resistance susceptibility phenotypic profiles obtained from the BV-BRC database[1].The pie chart on each country shows the proportion of resistance profiles for by class for each country, with the size of the chart indicating the overall number of genomes. The world map[2] has been divided according to the seven World Bank regions (East Asia and Pacific; Europe and Central Asia; Latin America and Caribbean; Middle East and North Africa; North America; South Asia; Sub-Saharan Africa).

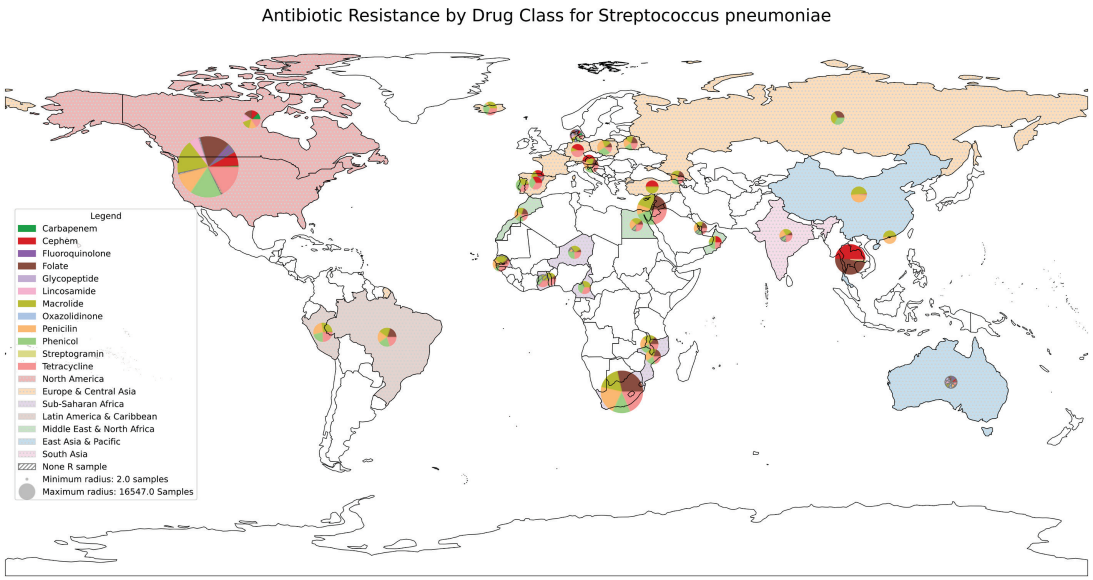

Figure S16. Geographic distributions of 13647 *S. pneumoniae* isolates with 52,756 associated resistance susceptibility phenotypic profiles obtained from the BV-BRC database[1].The pie chart on each country shows the proportion of resistance profiles for by class for each country, with the size of the chart indicating the overall number of genomes. The world map[2] has been divided according to the seven World Bank regions (East Asia and Pacific; Europe and Central Asia; Latin America and Caribbean; Middle East and North Africa; North America; South Asia; Sub-Saharan Africa).

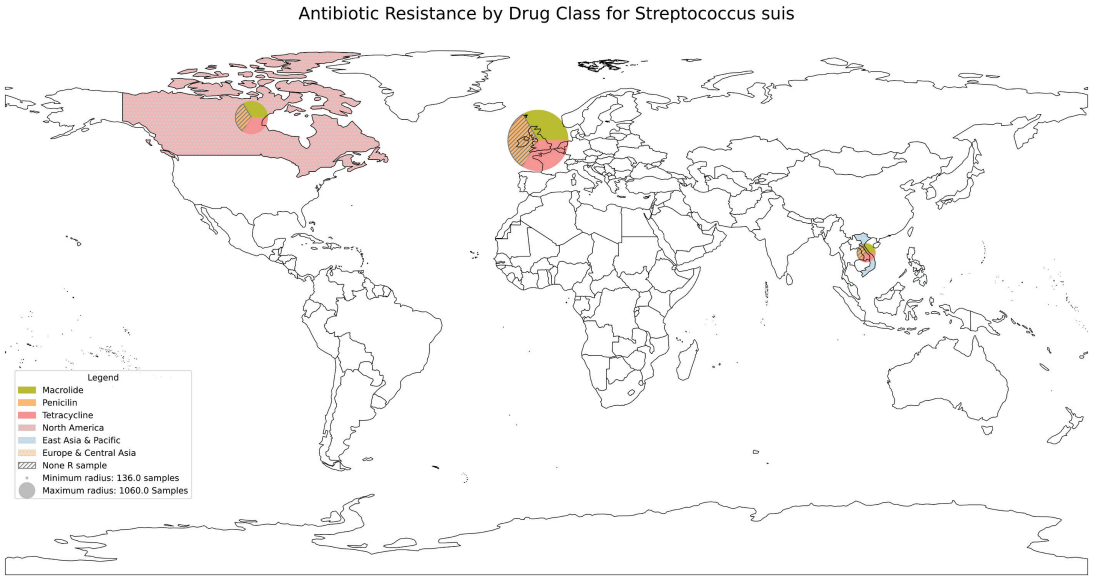

Figure S17. Geographic distributions of 550 *S. suis* isolates with 2,180 associated resistance susceptibility phenotypic profiles obtained from the BV-BRC database[1].The pie chart on each country shows the proportion of resistance profiles for by class for each country, with the size of the chart indicating the overall number of genomes. The world map[2] has been divided according to the seven World Bank regions (East Asia and Pacific; Europe and Central Asia; Latin America and Caribbean; Middle East and North Africa; North America; South Asia; Sub-Saharan Africa).

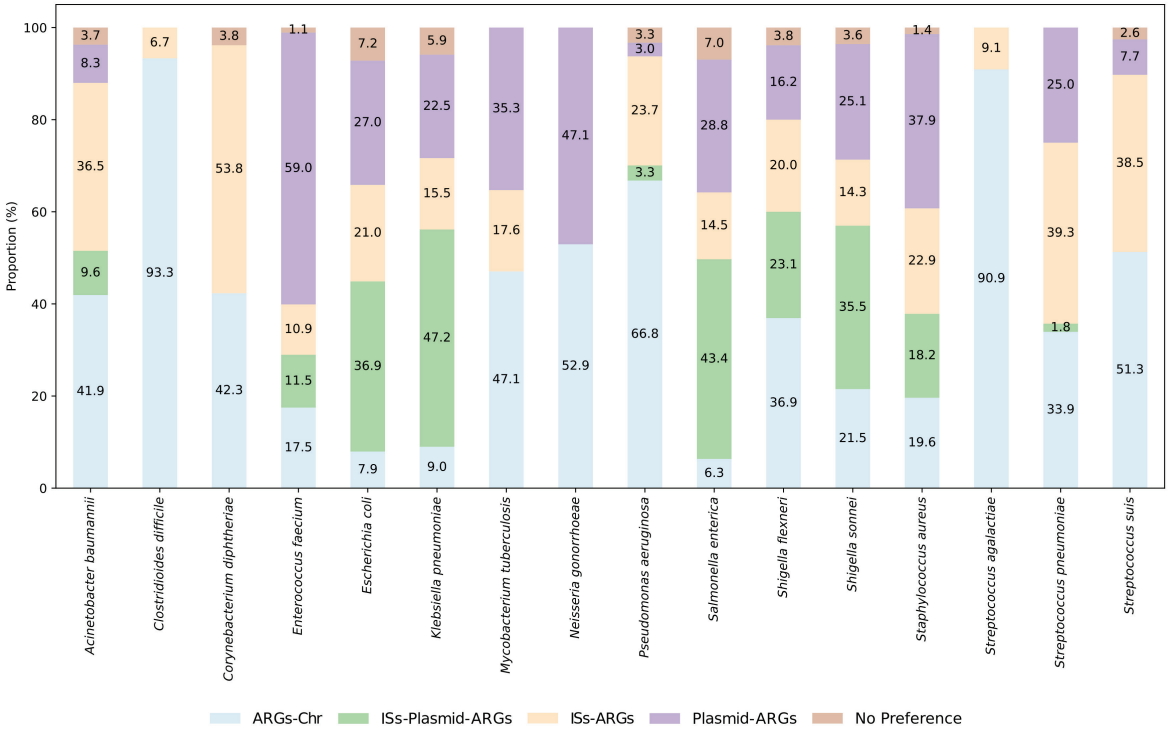

Figure S18. Stacked bar plot showing the proportion of AMR features and their predominant location across 16 bacterial species. Each feature can be present in four locations (ARG located in the chromosome = ARGs-Chr, ARG located in the chromosome and integrated within an IS = ISs-ARGs, ARG located in the plasmid and integrated within an IS = ISs-Plasmid-ARGs and ARGs present on plasmids but not within an insertion sequence = Plasmid-ARGs). The proportion of isolates carrying the feature at each location is given on **Supplementary Data 3**. If more than 50% of the isolates contain the feature in a specific location, this location is considered predominant, otherwise they are labelled as no preference.

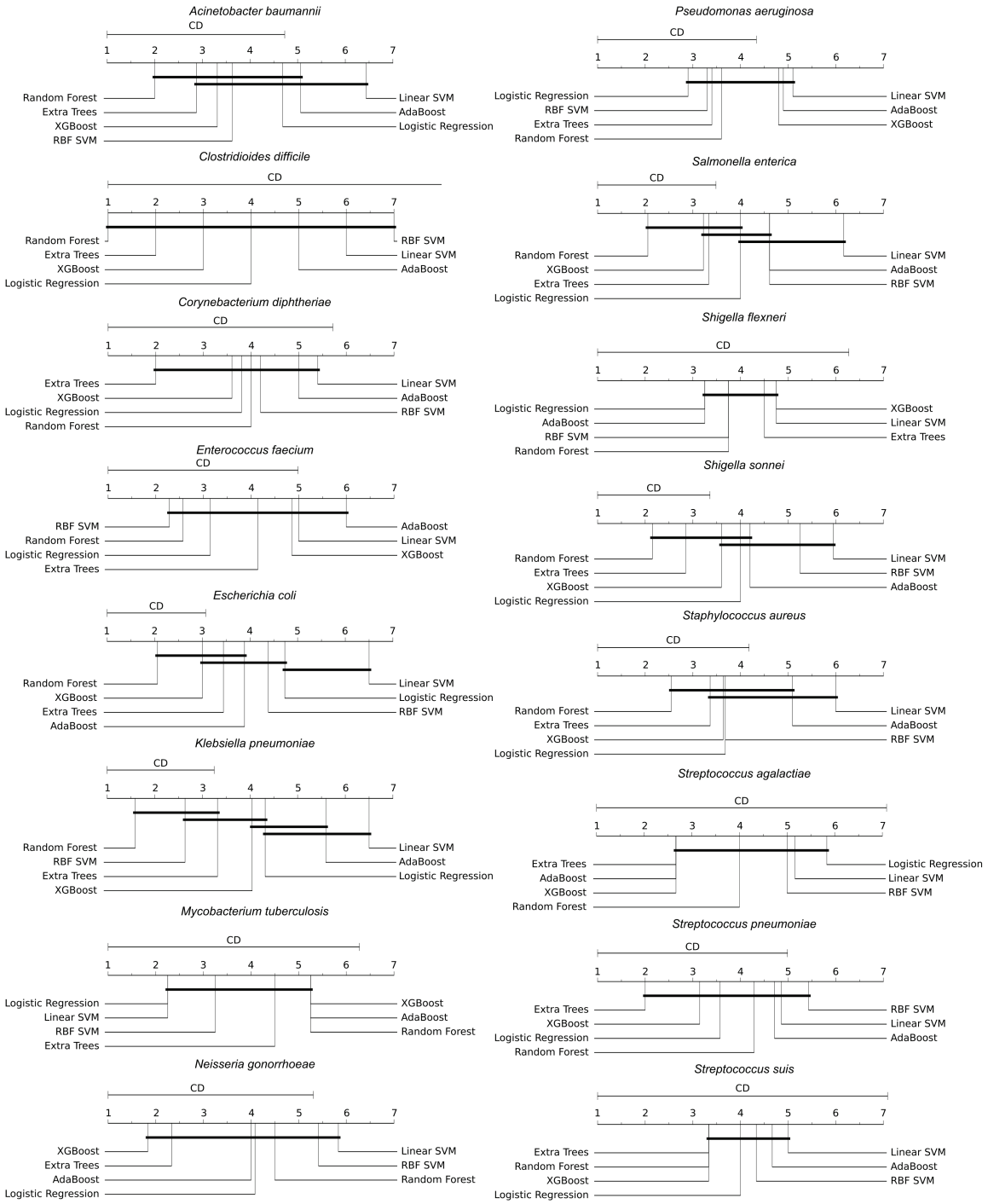

Figure S19. Nemenyi post-hoc tests. Comparison of the performance of the 7, using their average ordinal rank over the antibiotics analysed based on the AUC performance metric for the 16 bacterial species in this work. The x-axis indicates the average ordinal rank of the classifiers. The scale is from 1 (best rank) to 7 (worst rank). The ordinal rank of a classifier is defined as follows: the ML method with the best AUC is given rank 1, the second-best AUC rank 2 and the n-th AUC best rank n, with n being the number of classifiers used, with n equals to 7 in this study. Next, for each classifier, the ranks are averaged based on the number of antibiotics in each bacterial species. The critical distance (CD) is defined based on the Nemenyi post-hoc test, all the methods that fall in the same bold bar below the axis are considered statistically equivalent based on the CD value.

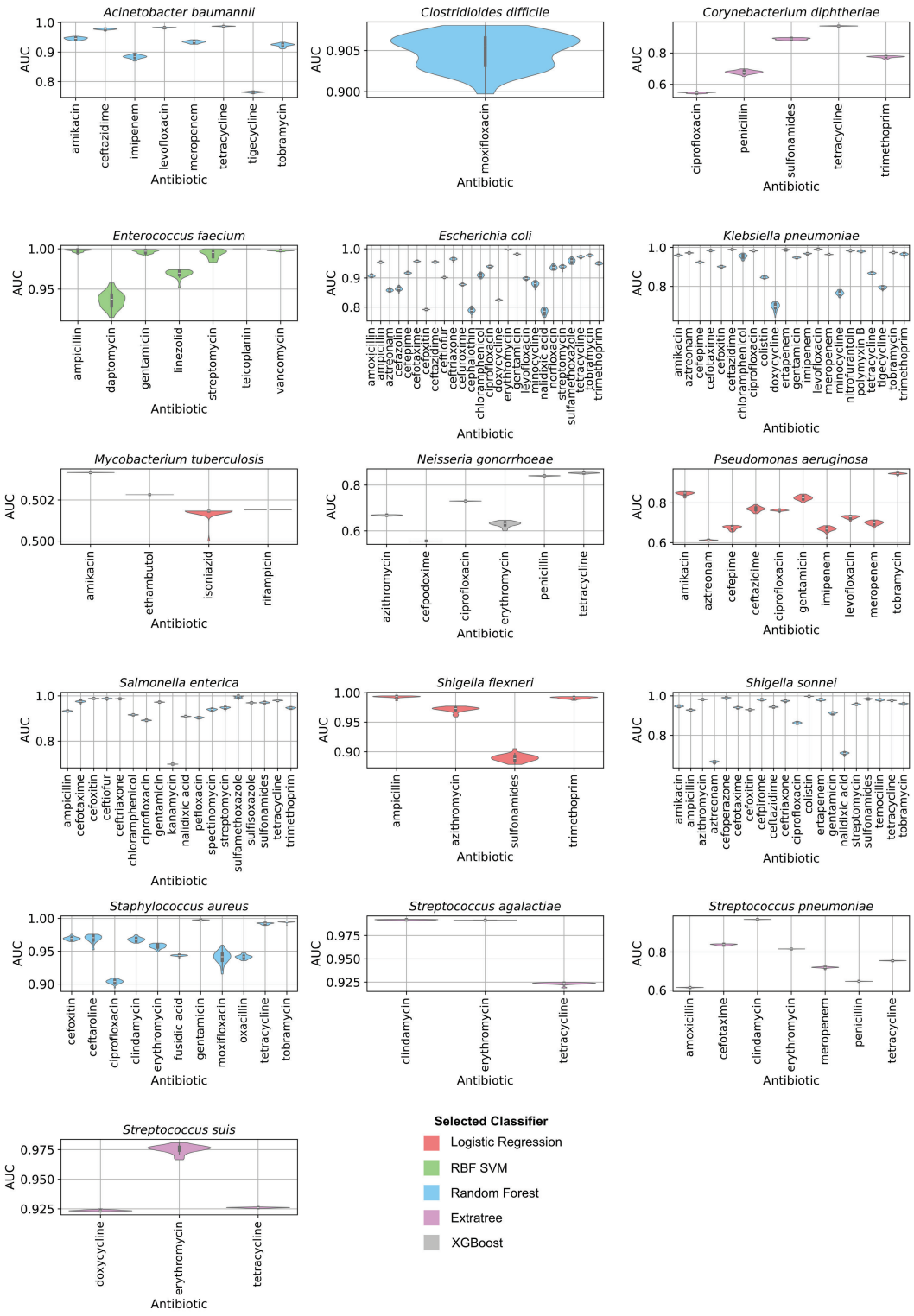

Figure S20. The supervised ML pipeline effectively predicts the resistance/susceptibility profiles of all 16 bacteria species. ML performance results are given for the area under the curve AUC, calculated from 30 training runs for each antimicrobial model. Plots as coloured according to the classifier used: logistic regression (red), RBF SVM (green), random forest (blue), ExtraTree classifier (purple) XGBoost (grey).

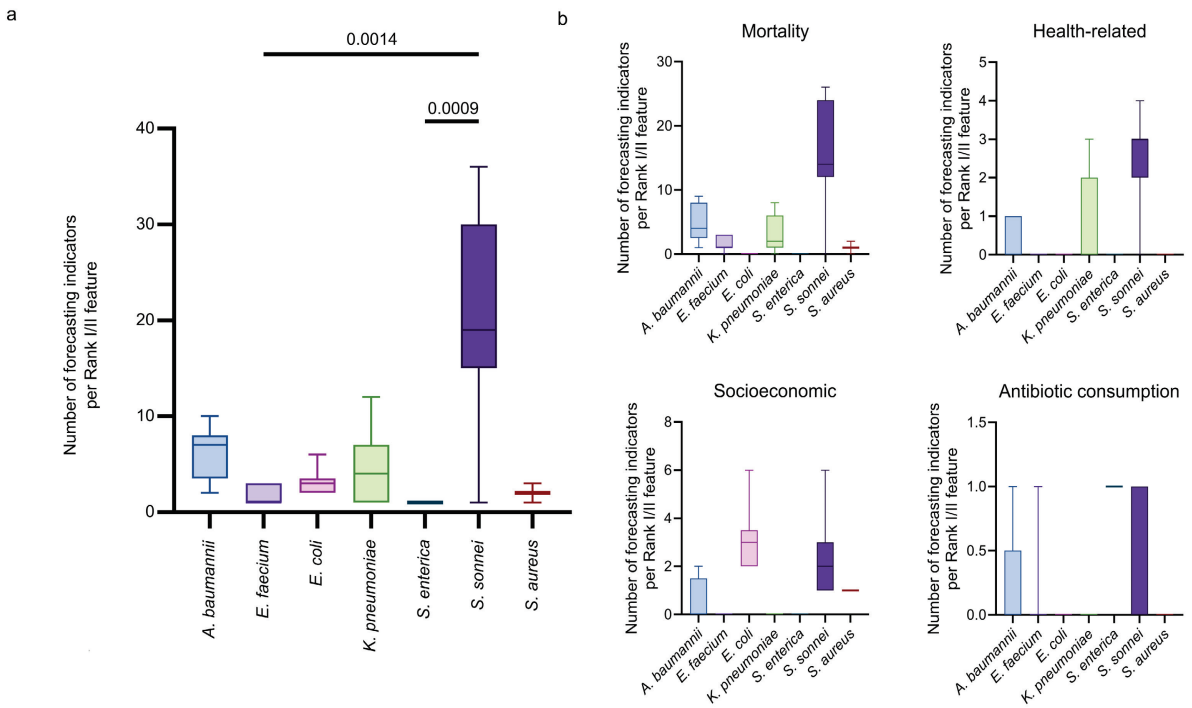

Figure S21. Number of increasing or stationary forecasting indicators per rank I/II genomic feature. (a) overall number of forecasting indicators per feature including antibiotic consumption, health-related, socioeconomic, environmental and mortality. Significant statistical differences shown as line with adjusted p-value above plot (Kruskal-Wallis, two tailed). (b) number of forecasting indicators per feature shown separately for antibiotic consumption, health-related, socioeconomic and mortality indicators. Environmental indicators not shown as no significant differences were overserved between species (Kruskal-Wallis, two tailed).

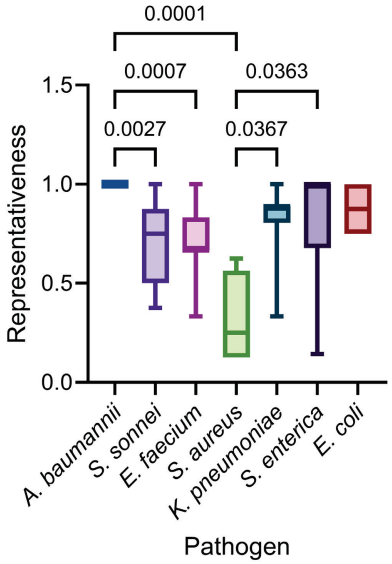

Figure S22. Boxplot of the representativeness of the selected rank I/II features across each pathogen relative to the ML models. For each pathogen we calculated a representativeness coefficient for the selected rank I/II features, as the number of classes in which the feature was selected divided by the number of classes in which the feature was present. For each pathogen, the box shows the interquartile range of the data with the median denoted by a horizonal line, and the whiskers indicate the range. Significantly different distributions are indicated on the plot with horizontal brackets and the adjusted p value given (Kruskal-Wallis, two-tailed)

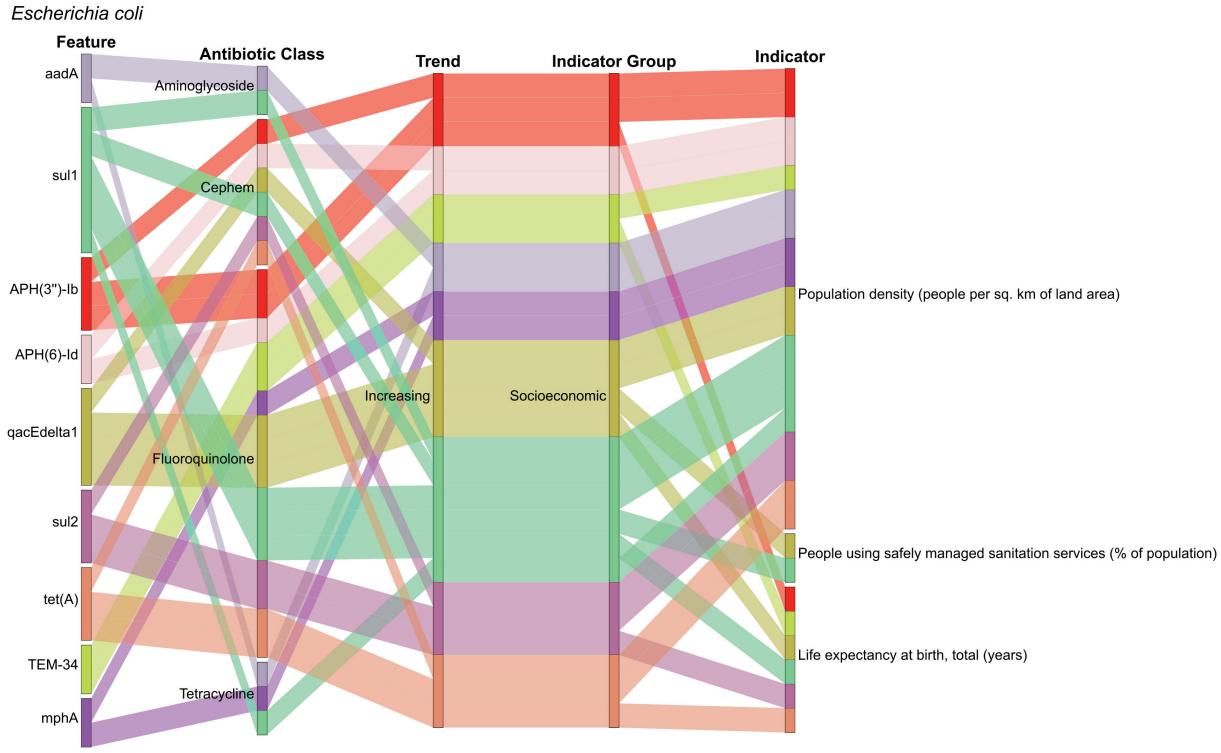

Figure S23. ***E. coli*** **Sankey flow diagram.** This Sankey diagram illustrates the relationships between AMR genomic features (feature), their associated antibiotic class identified via ML to each feature (Antibiotic class), the projected trend of each indicator (whether the indicator was forecasted to increased or remain stationary), indicator groups, and specific indicators (Indicator) within each group. Only rank I/II features associated with increasing indicators are displayed. The thickness of the links represents the number of different indicators, while the colours correspond to the associated genomic feature.

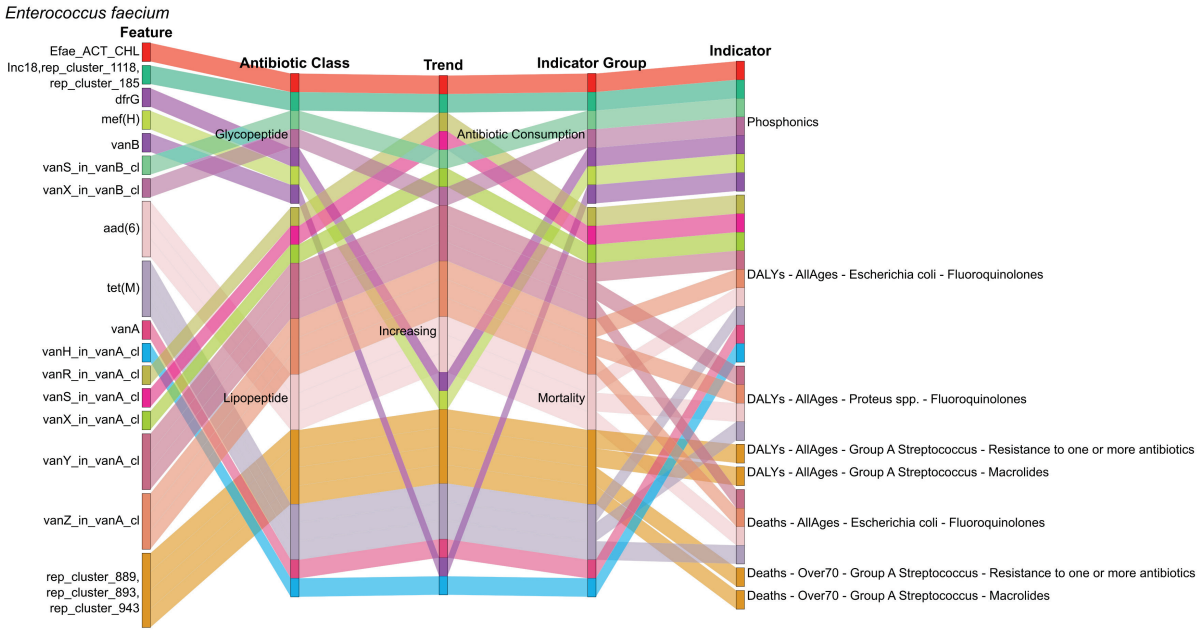

Figure S24. *E. faecium* Sankey flow diagram. This Sankey diagram illustrates the relationships between AMR genomic features (feature), their associated antibiotic class identified via ML to each feature (Antibiotic class), the projected trend of each indicator (whether the indicator was forecasted to increased or remain stationary), indicator groups, and specific indicators (Indicator) within each group. Only rank I/II features associated with increasing or stationary indicators are displayed. The thickness of the links represents the number of different indicators, while the colours correspond to the associated genomic feature.

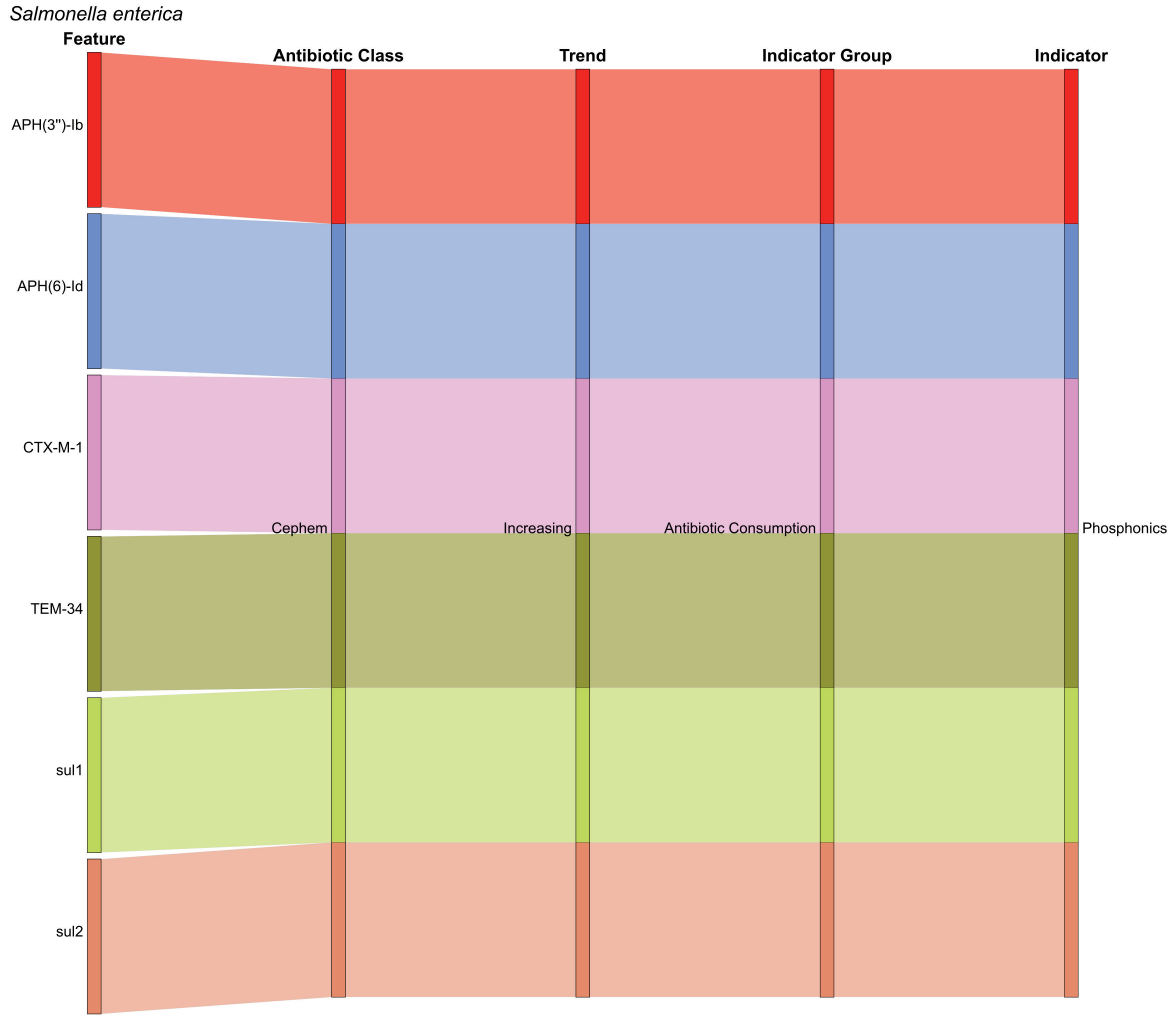

Figure S25. *S. enterica* Sankey flow diagram. This Sankey diagram illustrates the relationships between AMR genomic features (feature), their associated antibiotic class identified via ML to each feature (Antibiotic class), the projected trend of each indicator (whether the indicator was forecasted to increased or remain stationary), indicator groups, and specific indicators (Indicator) within each group. Only rank I/II features associated with increasing indicators are displayed. The thickness of the links represents the number of different indicators, while the colours correspond to the associated genomic feature.

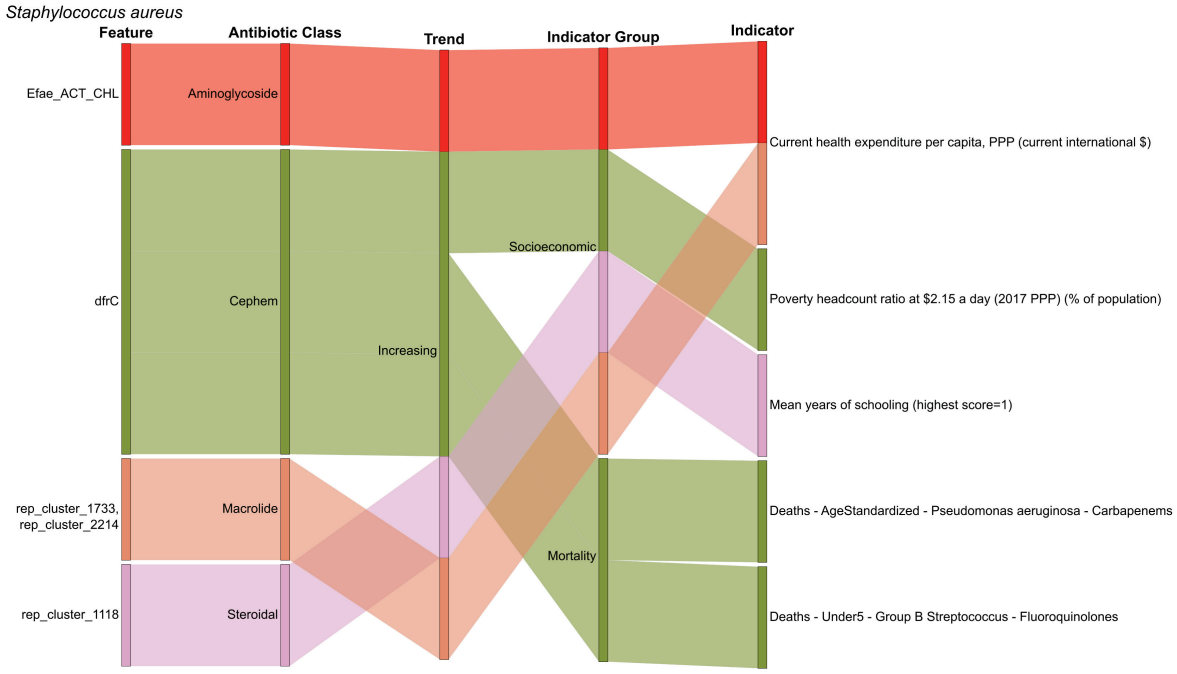

Figure S26. *S. aureus* Sankey flow diagram. This Sankey diagram illustrates the relationships between AMR genomic features (feature), their associated antibiotic class identified via ML to each feature (Antibiotic class), the projected trend of each indicator (whether the indicator was forecasted to increased or remain stationary), indicator groups, and specific indicators (Indicator) within each group. Only rank I/II features associated with increasing indicators are displayed. The thickness of the links represents the number of different indicators, while the colours correspond to the associated genomic feature.

Supplementary Data Legends

Supplementary Data 1 – Metadata of genomes – List of isolates with their corresponding BV-BRC genome ID accession. For each isolate, the following information is given: Bacterial species, additional accessions (where available), collection year, host name, isolation country, country code and presence/absence of CARD ARGs.

Supplementary Data 2 – List of Indicators – List of indicators from World Bank Data[3], ResistanceMap[4], Klein, et al.[5] and Meteostat data[6] and Global Health Data Exchange[7,8] including antibiotic consumption, social-economical, deaths, health-related and environmental risk factors collected from the same countries as the genomics data obtained from BV-BRC and across all available years.

Supplementary Data 3 – List of pathogen-feature pairs and their genomic location – List of pathogen-feature pairs indicating the distribution of the AMR features location as a percentage (ARG located in the chromosome = ARGs-Chr, ARG located in the chromosome and integrated within an IS = ISs-ARGs, ARG located in the plasmid and integrated within an IS = ISs-Plasmid-ARG and ARGs present on plasmids but not within an insertion sequence = Plasmid-ARGs) across all isolates for each bacterial species.

Supplementary Data 4 – ARGs present in multiple genomic locations within a single isolate. Bacterial species, genome ID, ARG name, gene location (ARG located in the chromosome = ARGs-Chr, ARG located in the chromosome and integrated within an IS = ISs-ARGs, ARG located in the plasmid and integrated within an IS = ISs-Plasmid-ARG and ARGs present on plasmids but not within an insertion sequence = Plasmid-ARGs), contig ID, plasmid type (where applicable) and MGE name (where applicable) are given.

Supplementary Data 5 – Machine Learning performance indicators - Machine learning performance for each of the 7 classification methods used for the 16 bacteria species correlating the genetic features to the resistance/susceptibility against a panel of antimicrobials for each individual bacteria species. The performance metrics were accuracy (TP+TN/(P+N)), sensitivity (true positive rate: TP/P), specificity (true negative rate: TN/N), AUC, precision and Cohen's Kappa score. The scores for each performance metric were computed from 30 simulations using nested cross-validation. The mean ± standard deviation of these 30 iterations was then used as the result statistics for the performance.

Supplementary Data 6 – ML-selected features in models with performance over 90% AUC – Features correlated to resistant-susceptibility profiles selected by the machine learning on models with an AUC over 90% in 14 of the 16 bacterial species. For each pathogen-feature pair, the following information is given: percentage of isolates carrying the feature in a mobile element; countries where these isolates were found, their corresponding World Bank regions,; years of sample isolation, hosts in which they were found, human enrichment as a fold change, bacterial species carrying the feature, bacterial species where the ML identified the genotype-phenotype association with AUC over 90%, ESKAPE/WHO high/critical priority information and number of antibiotic classes where ML identified the association.

Supplementary Data 7 – Pearson correlation tables for each indicator-feature pair – Pearson correlation coefficients and p-value statistics for each indicator-feature pair (Pearson correlation $r > |0.5|$, $p < 0.05$).

Supplementary Data 8 – Increasing indicator-feature pairs, considering features where the feature prevalence is increasing – List of feature-indicator pairs strongly correlated (Pearson correlation $r > |0.5|$, $p < 0.05$) with the indicator forecasted to increase by 2050. For each feature-indicator pair the following information is given: the number of isolates, countries and years used for the forecasting analysis; the trend analysis performed for both the indicator and the feature forecasting using ADF (Augmented Dickey-Fuller) and KPSS (Kwiatkowski-Phillips-Schmidt-Shin) test statistics with a confidence level of 95% for each one.

Supplementary Data 9 – Stationary indicator-feature considering features where the feature prevalence is increasing – List of feature-indicator pairs strongly correlated (Pearson correlation $r > |0.5|$, $p < 0.05$) with the indicator forecasted to be stationary by 2050. For each feature-indicator pair the following information is given: the number of isolates, countries and years used for the forecasting analysis; the trend analysis performed for both the indicator and the feature forecasting using ADF (Augmented Dickey-Fuller) and KPSS (Kwiatkowski-Phillips-Schmidt-Shin) test statistics with a confidence level of 95% for each one.

Supplementary Data 10 – Decreasing indicator-feature considering features where the feature prevalence is increasing – List of feature-indicator pairs strongly correlated (Pearson correlation $r > |0.5|$, $p < 0.05$) with the indicator forecasted to decrease by 2050. For each feature-indicator pair the following information is given: the number of isolates, countries and years used for the forecasting analysis; the trend analysis performed for both the indicator and the feature forecasting using ADF (Augmented Dickey-Fuller) and KPSS (Kwiatkowski-Phillips-Schmidt-Shin) test statistics with a confidence level of 95% for each one.

Supplementary Data 11 – Ranking of the features correlated to indicators increasing and stationary – List of the increasing or stationary features (i.e. indicators that were forecast to increase or remain stationary over time) ranked as I, II, III, or IV. The framework consists of a decision tree based on three criteria: (1) enrichment in human isolates; (2) gene mobility; (3) presence/absence in ESKAPE pathogens or WHO critical/high pathogens lists (see **Methods**).

Supplementary Data 12 – Population structure - Standard association index (I^S_A) to measure for clonality in the population at whole cohort level and at ST type level for each bacterial species.

Supplementary Notes

Supplementary Note 1

Escherichia coli

E. coli carried a total of 9 rank I/II features, which were linked to three increasing indicators associated to four antibiotic drug classes by the ML models: cephems, fluoroquinolones, tetracyclines, and aminoglycosides. Fluoroquinolones were the most frequently associated with these features (**Fig. S23**).

All the associated indicators were socioeconomic, with population density being the most common predictor, forecasting an increase in the prevalence of all nine features.

Enterococcus faecium

In *E. faecium*, 17 rank I/II features selected by two different antibiotic classes (glycopeptides (7 features), and lipopeptides (ten features)) were predicted to increase in prevalence, driven by eight rising indicators. Seven of these indicators were mortality indicators while one was antibiotic consumption (phosphonic).

Notably, seven rank I/II features (*Efae_ACT_CHL, dfrG, vanB, mef(H), vanXB, vanSB, Inc18, rep_cluster_1118, rep_cluster_185*) associated to glycopeptide resistance by the machine learning models were linked to phosphonic acid antibiotic consumption (**Fig. S24**). Three of these features (*vanB, vanXB, and vanSB*) are well-known for their association with vancomycin resistance.

Salmonella enterica

In *S. enterica*, six rank I and II features were identified as correlated to resistance across seven different antibiotic classes by the ML models (aminoglycoside, cephem, fluoroquinolone, folate, penicillin, phenicol, and tetracycline*)*. However, all six features were specifically associated with an increase in phosphonic antibiotic consumption by the global data indicators, **Fig. S25**.

Staphylococcus aureus

Four rank I/II features were analysed in relation to *Staphylococcus aureus*, all of which were associated with rising mortality and socioeconomic indicators (**Fig. S26**). Notably, the trimethoprim-resistance gene *dfrC*—selected exclusively in *S. aureus*—was linked to both mortality indicators and poverty headcount. Additionally, its association with mortality indicators across multiple bacterial species suggests a potential role in co-infection.

Supplementary Note 2

The genomic context of the resistance determinants varied among bacterial species. For instance in carbapenem resistant *A. baumanii*, *APH(3'')-Ib, APH(6)-Id* were primarily IS-associated and integrated in the chromosome. These results are in line with *A. baumannii* known to acquire resistance through IS

elements[9,10], and highlight the crucial role of clinical settings in contributing to this acquisition. Conversely, when present in 3rd-generation cephalosporin and fluoroquinolone resistant *E. coli*, *S. sonnei* and *S. enterica*, these same features were mostly found on plasmids and not IS-associated. More generally, within the 78 rank I/II feature-pathogen pairs, *A. baumannii* features were predominantly IS-associated and in chromosome, geographically confined and mainly and associated with health-related and mortality indicators, further suggesting a strong associated with clinical settings. Conversely, *in E. coli*, *S. sonnei* and *S. enterica*, the 78 features were primarily plasmid-associated, without ISs links, widespread and all linked to antibiotic consumption (phosphonic). Phosphonic is an antibiotic class widely used in livestock production (particularly in Asia and Latin America)[9] and for which resistance in *S. enterica* is becoming a serious health concern[11]. This suggests livestock production as a key driver of plasmid encoded resistance in these species. The different genomic contexts (IS- vs. plasmid-associated) suggest divergent selective pressures operated by external factors on the genomes and the importance of tracking both mobile and chromosomal AMR elements to understand their future transmission dynamics fully[12,13]. These results indicate environment/health-related pressures shaping the genomic make-up of AMR and its dissemination. In our data it emerges that plasmid-associated AMR genes are not only globally widespread but also concentrated in high-income, high-density regions, whereas IS- and transposon-associated resistance elements follow a region-specific distribution linked to socioeconomic vulnerabilities.

Host distribution patterns revealed most of these features were multi-host, but five — *APH(3')-Ia*, *ermB*, *aadA2*, *tet(M)*, and rep_cluster_1118 in *A. baumannii*, *E. coli*, *E. faecium*, *K. pneumoniae*, *S. aureus*, *S. enterica* and *S. sonnei* — were mainly in humans and food animals, suggesting a strong association with antibiotic use in clinical and agricultural settings. All the five features were found in East Asia and the Pacific, Europe and Central Asia, and North America. Additionally, *rep_cluster*_1118 was also present in sub-Saharan Africa while *APH(3')-Ia*, *aadA2* were found worldwide. All five features were associated with various antibiotic classes, with aminoglycosides resistance common to all. Aminoglycosides, classed by WHO as critically important antibiotics[14] are widely used clinically[15] and usage in food animals has been highlighted as a concern in both Africa[16] and Asia[17]. Furthermore aminoglycoside-resistant *K. pneumoniae* was considered one of the top ten pathogen-drug combinations in Africa in the global burden of disease estimates[18].

References

1 BV-BRC. *The Bacterial and Viral Bioinformatics Resource Center (BV-BRC)*, < https://www.bv-brc.org/> (Last accessed 26-09-22

2 Natural Earth. *Natural Earth Data*, <https://www.naturalearthdata.com/> (2024). Last accessed

3 World Bank Group. *World Bank Open Data*, <https://data.worldbank.org/> (2024). Last accessed 01/09/2024

4 OneHealthTrust. *ResistanceMap:AntibioticUse*, <https://resistancemap.onehealthtrust.org/AntibioticUse.php> (2024). Last accessed 01/09/2024

5 Klein, E. Y. *et al.* Global trends in antibiotic consumption during 2016–2023 and future projections through 2030. *Proceedings of the National Academy of Sciences* **121**, e2411919121, doi:doi:10.1073/pnas.2411919121 (2024).

6 Lamprecht, C. S. *Meteostat Python v1.2.0*, <https://github.com/meteostat/meteostat-python> (2024). Last accessed 01/09/2024

7 Institute for Health Metrics and Evaluation (IHME), U. o. O. Global Burden of Disease Study 2021 (GBD 2021) Bacterial Antimicrobial Resistance Burden Estimates 1990-2021 and Forecasts 2022-2050. *Seattle, United States of America: Institute for Health Metrics and Evaluation (IHME), 2024.* (2024).

8 University of Oxford & University of Washington. *Deaths - Institute for Health Metrics and Evaluation (IHME) MICROBE*, <https://vizhub.healthdata.org/microbe> (2024). Last accessed 01/09/2024

9 Vijayakumar, S. *et al.* Insertion sequences and sequence types profile of clinical isolates of carbapenem-resistant A. baumannii collected across India over four year period. *Journal of Infection and Public Health* **13**, 1022-1028, doi:https://doi.org/10.1016/j.jiph.2019.11.018 (2020).

10 Jeon, J. H., Jang, K.-M., Lee, J. H., Kang, L.-W. & Lee, S. H. Transmission of antibiotic resistance genes through mobile genetic elements in Acinetobacter baumannii and gene-transfer prevention. *Sci. Total Environ.* **857**, 159497, doi:https://doi.org/10.1016/j.scitotenv.2022.159497 (2023).

11 Monte, D. F. M., Doi, Y. & Lincopan, N. High prevalence and global distribution of fosfomycin resistance genes in Salmonella serovars. *The Lancet Microbe* **4**, e968, doi:10.1016/S2666-5247(23)00261-6 (2023).

12 Djordjevic, S. P. *et al.* Genomic surveillance for antimicrobial resistance — a One Health perspective. *Nature Reviews Genetics* **25**, 142-157, doi:10.1038/s41576-023-00649-y (2024).

13 Castañeda-Barba, S., Top, E. M. & Stalder, T. Plasmids, a molecular cornerstone of antimicrobial resistance in the One Health era. *Nature Reviews Microbiology* **22**, 18-32, doi:10.1038/s41579-023-00926-x (2024).

14 World Health Organization. *WHO List of Medically Important Antimicrobials: a risk management tool for mitigating antimicrobial resistance due to non-human use*. (World Health Organization, 2024).

15 Becker, B. & Cooper, M. A. Aminoglycoside antibiotics in the 21st century. *ACS Chem. Biol.* **8**, 105-115 (2013).

16 Kimera, Z. I., Mshana, S. E., Rweyemamu, M. M., Mboera, L. E. G. & Matee, M. I. N. Antimicrobial use and resistance in food-producing animals and the environment: an African perspective. *Antimicrob Resist Infect Control* **9**, 37, doi:10.1186/s13756-020-0697-x (2020).

17 Harun, A. B., Khatri, B. & Karim, M. R. Phenotypic and genotypic patterns of antimicrobial resistance in livestock and poultry in South Asia: A systematic review and meta-analysis. *Food Control* **164**, 110575, doi:https://doi.org/10.1016/j.foodcont.2024.110575 (2024).

18 Naghavi, M. *et al.* Global burden of bacterial antimicrobial resistance 1990–2021: a systematic analysis with forecasts to 2050. *The Lancet* **404**, 1199-1226, doi:https://doi.org/10.1016/S0140-6736(24)01867-1 (2024).